PROCEEDINGS, 49th Workshop on Geothermal Reservoir Engineering
Stanford University, Stanford, California, February 12-14, 2024
SGP-TR-227

Insights on the Water Produced from a Vapor-Dominated System at Patuha Geothermal Field, Indonesia

Hendy Sujarmaitanto, Andrian P.Wardana, Chevy Iskandar, Rhyno S.Sesesega and M.Istiawan Nurpratama

PT. Geo Dipa Energi, Aldevco Octagon 2nd Floor. Jl. Warung Jati Barat No.75 South Jakarta 12740 - Indonesia

hendy.s@geodipa.co.id

Keywords: Patuha geothermal field, vapor-dominated system, geochemistry, steam-condensate layer, scaling, deep reservoir brine.

ABSTRACT

The Patuha geothermal field is one of the few vapor-dominated geothermal systems in the world. Up to this point, brine reservoirs have not been confirmed in existing production wells. However, some wells in Patuha showed the presence of liquid, which is visually observed through the sampling port at the bottom during routine geochemical sampling, as seen in wells HND-A and HND-C. This condition has also been confirmed through the Tracer Flow Test (TFT), where the well has a dryness of 95%-98% with a slight liquid fraction. The results of PT logging surveys in both of these wells confirm the presence of a liquid column inside the wellbore. Unexpectedly, well HND-B, which appeared to be in dry-steam conditions at the surface, also shows the same condition. To obtain representative liquid chemistry data, further confirmation is conducted by running a liquid Downhole Sampling (DHS). The analysis results of water samples from wells HND-A and HND-C are secondary water products, with a predominant SO_4 content. However, these two samples have slight differences in their chemistry. The sample from HND-A has a relatively lower pH value, higher levels of SO_4, SiO_2, and Fe, and lighter stable isotope values compared to the sample from HND-C. In contrast, well HND-B represents a different chemistry compared to the two previous samples, with the results of the anion diagram plot indicating a shift towards the Cl water area. This evaluation is carried out to gain an understanding of the processes and the origin of this water in the Patuha geothermal field.

1. INTRODUCTION

The Patuha geothermal field is one of the few vapor-dominated geothermal systems in the world. Since the Commercial Operation Date (COD) in September 2014, the field has been operating for about 9 years with an installed capacity of 1 x 55 MW. The field is located in Pangalengan Geothermal Concession Area Crop Out, West Java Province of Indonesia, around 50 km to the southwest of Bandung, and developed by state-owned company PT. Geo Dipa Energi (Persero) (Figure 1). Exploration drilling activity was started in 1996 with a slim hole, temperature core hole (TCH) and continued field development with drilling of big hole wells in 1997 for production and injection wells by Patuha Power Ltd before it was stopped in 1998 due to the Indonesian economic crisis.

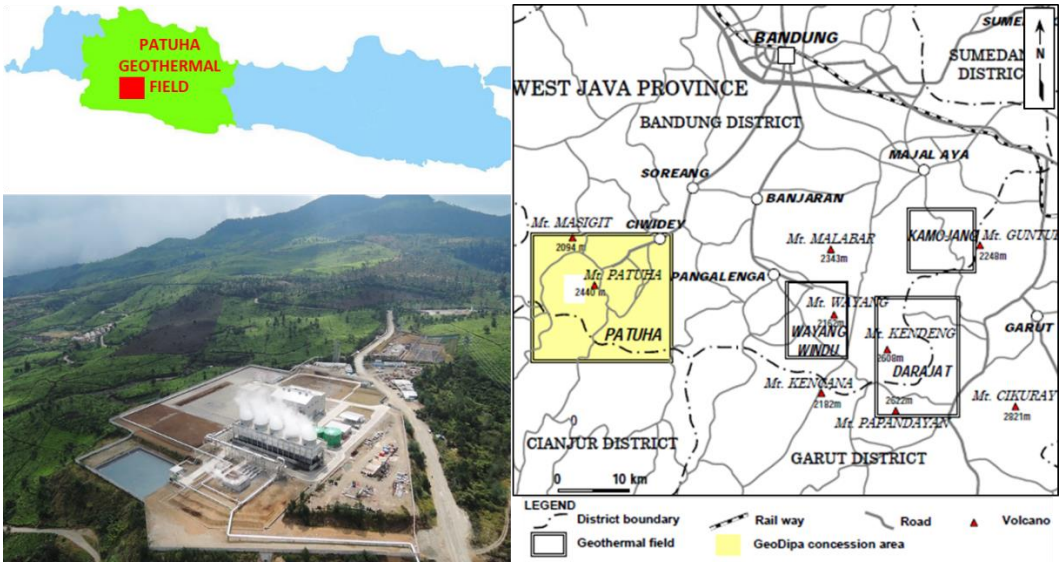

Figure 1: Location of the Patuha geothermal field.

The initial geochemical data for Patuha were collected during the welltest period between 1997 and 1998. Following a period of idle activity for more than 15 years, the geochemical monitoring program, utilizing an external laboratory, commenced in 2014 when Unit 1 Patuha began operations with contributions from 7 production wells, including HND-A. At that time, the scope of the geochemical monitoring program was limited to gas sample collection. Subsequently, from 2015 to 2021, the external geochemical monitoring program evolved into a comprehensive annual process on all production wells contributing to the generation of Unit 1 Patuha. Monitoring expanded beyond gas samples to include steam condensate (SCS) and separated water (SPW) samples, visible in some production wells through bottom port sampling. Stable isotope sampling supported geochemical interpretation in Patuha. For a holistic evaluation, monitoring extended from upstream to downstream, including steam purity sampling on the main steam line. Additionally, Tracer Flow Tests (TFT) were performed, especially on wells with water fractions, to determine dryness, enthalpy values, and flow rates. As of 2021, 10 production wells undergo routine geochemical monitoring, including HND-A, HND-B & HND-C (Figure 2). Since Patuha is a vapor-dominated system, routine monitoring of surface superheat is also conducted, especially on wells producing dry steam.

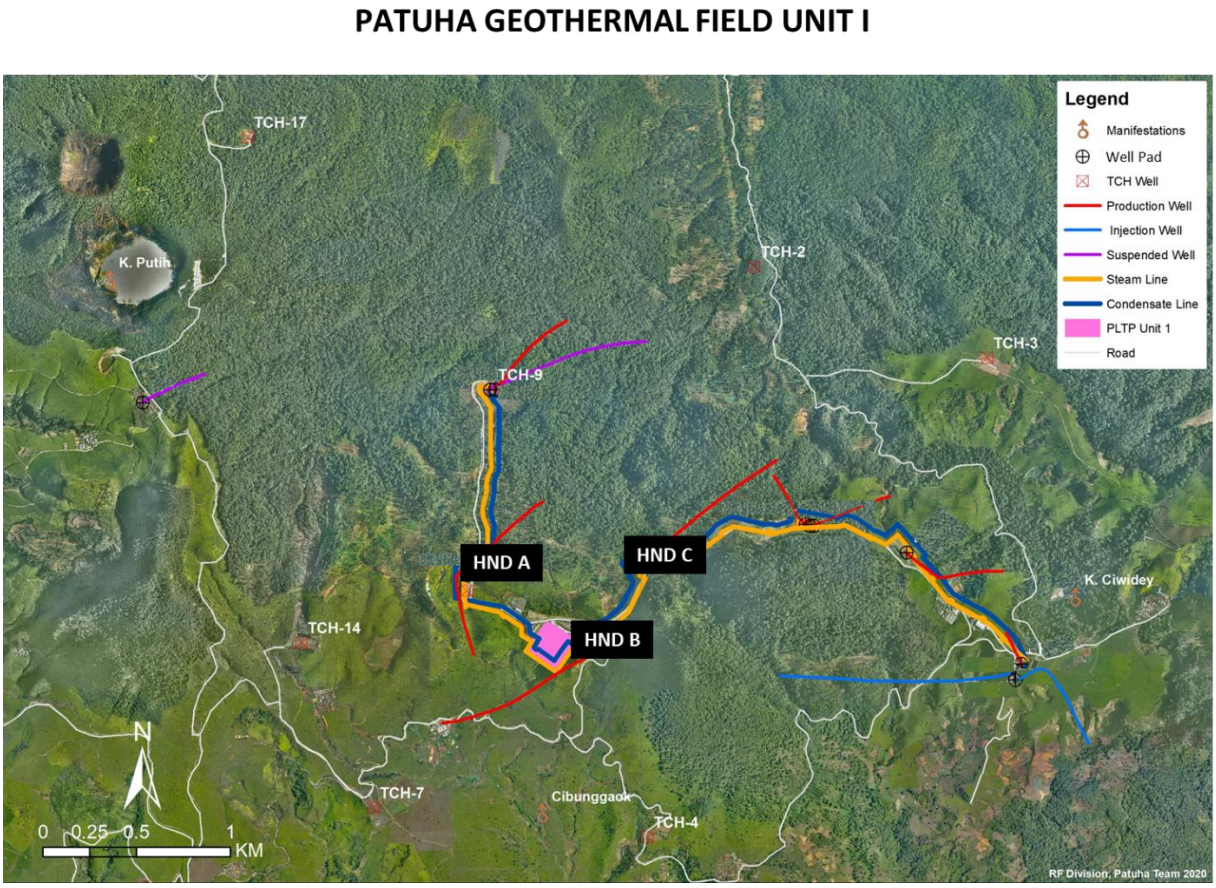

Figure 2: Map showing the Patuha Geothermal Field Unit 1, highlighting the locations of HND-A, HND-B & HND-C.

Up to this point, brine reservoirs have not been confirmed in existing production wells. However, some wells in Patuha have shown the presence of liquid, which is visually observed through the sampling port at the bottom during routine geochemical sampling, as seen in wells HND-A and HND-C. This condition has also been confirmed through the Tracer Flow Test (TFT), well has a dryness of 95%-98% with a slight liquid fraction. In fact, well HND-A previously showed a dryness value of around 50%. The results of PT logging surveys in both of these wells confirm the presence of a liquid column inside the wellbore. Unexpectedly, well HND-B, which appeared to be in dry-steam conditions at the surface, also shows the same condition. This condition was initially identified through consistent Pressure & Temperature (PT) logging survey results indicating a liquid column inside the wellbore. Until 2021, these three wells showing the presence of liquid require special attention, especially from a geochemical perspective, to determine the type and origin of the water. To obtain representative liquid chemistry data, further confirmation is conducted by running a liquid Downhole Sampling (DHS). It is expected that sampling water directly at the suspected depth of influx or liquid column will eliminate uncertainties compared to sampling water that has traveled to the surface facility.

2. LIQUID PRESENCE

The discussion in this study will focus solely on the three wells that have been previously discussed, namely HND-A, HND-B, and HND-C. Each well will be elaborated based on the history and evidence found regarding the presence of liquid. Data integration is carried out in this evaluation, incorporating information from Pressure & Temperature (PT) logging surveys, Downhole Video (DHV), Downhole Sampling (DHS), and geochemical analysis.

2.1 Presence of water in HND-A

Well HND-A was drilled in 1997 but was not utilized for commercial production until 2014. Since the initial production, HND-A has been producing a two-phase fluid, which is very uncommon for a vapor-dominated system like the Patuha geothermal field. A Pressure, Temperature & Spinner (PTS) logging survey in flowing condition was conducted in September 2015, revealing a decrease in temperature and a change in reaction from the spinner data (with rotations much higher than the previous trend). Based on simulation results, casing leakage is suspected at a depth of ±163 mMD. Therefore, a decision was made in February 2016 to immediately install a separator to overcome water carryover in the production fluid.

As a follow-up to the PTS survey analysis results in 2015, it was decided in August 2018 to conduct a Magnetic Thickness Detector (MTD) survey and Downhole Video (DHV) to gain a better understanding of the casing conditions in this well. The MTD survey was conducted to a depth of 855 mMD with the objective of determining the integrity of the 13-3/8" production casing using average metal loss data per depth. The MTD survey results showed intentional corrosion in the 13-3/8" casing with 47.2% at 161.5 mMD and intentional corrosion in the 20" casing with 26.7% at 163.9 mMD. Based on these results, it is suspected that cold water influx is occurring laterally from the formation into the wellbore (Figure 3).

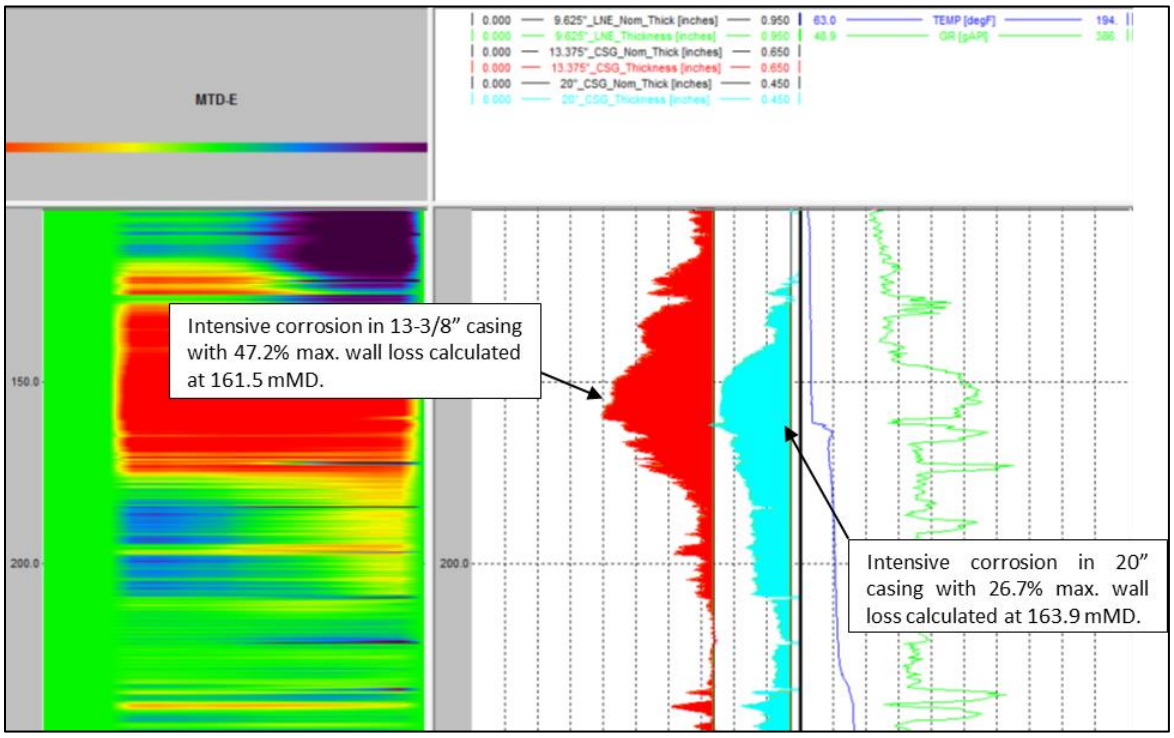

Figure 3: Wall thickness profile of the intermediate casing 20" and production casing 13-3/8" from 100 mMD to 250 mMD.

The Downhole Video survey (DHV) aims to provide a clearer visual of the wellbore condition, especially in the casing section that shows intensive corrosion from the Magnetic Thickness Detector (MTD) survey results. The DHV results did not indicate any leakage at a depth of 161.5 mMD, which previously showed intensive corrosion of 47.2%. However, casing leakage was found at a depth of 163.55 mMD with intensive corrosion of 45.7%. These observations further support the casing leakage scenario, where cold water enters laterally from the formation, passes through the 20" conductor casing, and then enters the wellbore through the 13-3/8" production casing (Figure 4).

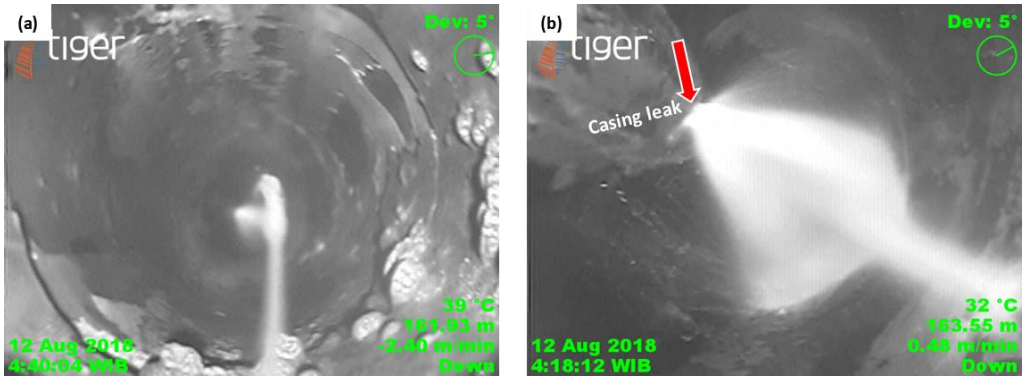

Figure 4. Downhole video survey: (a) Casing condition at depth of 161.5mMD, (b) Casing condition at depth of 163.55mMD.

The results of the Tracer Flow Test (TFT) measurements indicate that the dryness value of well HND-A is approximately 50%, meaning half of it is due to cold water influx resulting from casing leakage. Therefore, the enthalpy of this well is also the lowest, ranging from 1.749 to 1.836 kJ/kg, compared to other Patuha production wells that range above 2.500 kJ/kg. The analysis of separated water (SPW) samples taken from bottom port sampling indicates that the produced water is groundwater with a characteristic magnesium (Mg) value ranging from 3 to 4 ppm. Consequently, based on the results of several surveys and analyses, it was decided to conduct a Workover using a 75 HP rig in October 2020 with the main objectives being (1) Cement Plug & Squeeze cementing for remedial 13-3/8" Casing leak at 163 mMD and (2) Set 9-5/8" Casing (long string) to 775 mMD (9-5/8" Top of Liner) and cement to secure and maintain the lifetime well due to well integrity issues. Therefore, after the workover, the tie-back casing configuration of well HND-A became as shown in Figure 5.

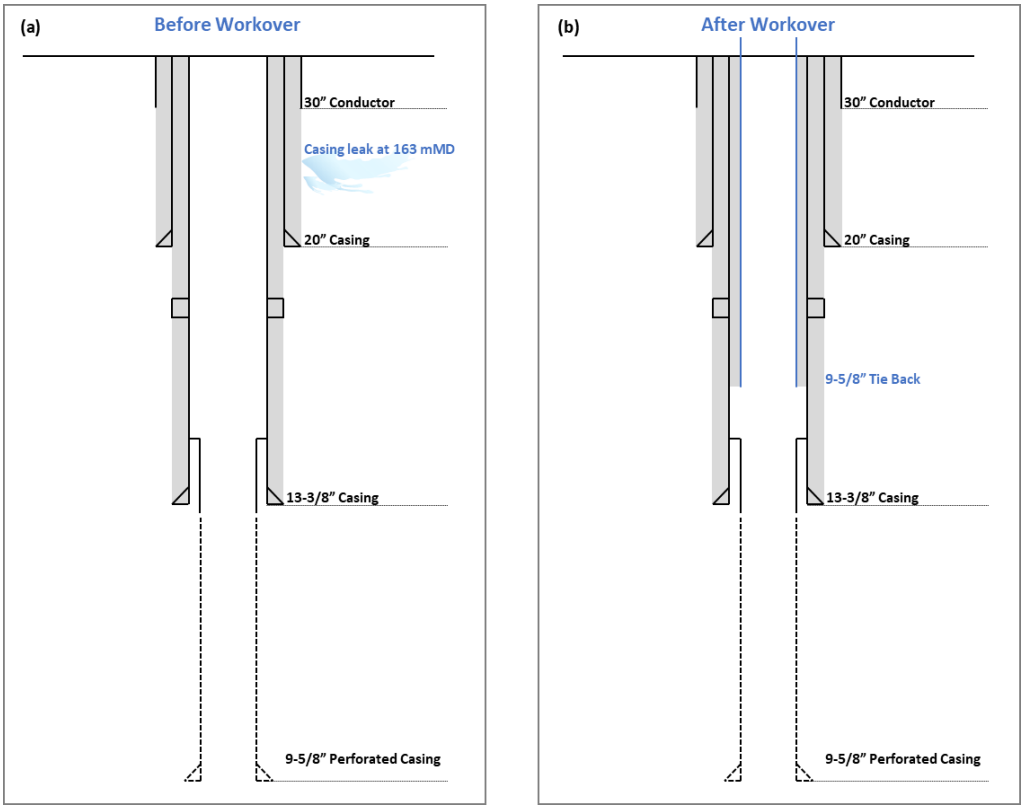

Figure 5. Well Schematic of HND-A: (a) Before Workover, (b) After Workover.

The workover by casing milling, remedial cementing, and casing-reline is expected to address the shallow groundwater intrusion problem. Proven after the tie-back casing 9-5/8" workover, the Tracer Flow Test (TFT) results show an increase in the dryness of well HND-A to around 99%, with an enthalpy of approximately 2.751 kJ/kg. Therefore, with the well now in a dry condition, the use of the production separator is no longer needed and can be removed. Below is a comparison of the TFT results for well HND-A before and after the workover (Table 1).

Table 1. HND-A TFT Results Comparison (Before and After Workover).

Location	Date	FCV (%)	WHP		Steam Rate TFT	Liquid Rate TFT	Enthalpy	TMF	Steam Fraction	Liquid Fraction	Remarks
			psig	barg	t/h	t/h	kJ/kg	t/h			
HND-A	21/02/2018	100	120	8.3	24.4	24.9	1749	49.3	0.50	0.51	With Sep. Prod (Before WO)
	24/09/2019	100	120	8.3	29.3	24.7	1836	54.0	0.54	0.46	
	09/09/2020	100	110	7.6	27.2	24.2	1809	51.5	0.53	0.47	
	30/03/2021	50	119	8.2	26.6	0.3	2751	26.9	0.99	0.01	Without Sep. Prod (After WO)

The post-workover geochemical monitoring program indicates the continued presence of separated water (SPW) samples from bottom port sampling. However, the encountered water exhibits characteristics of condensate with a very dilute concentration. This condensate is suspected to form as steam flows from within the wellbore towards the surface. In June 2021, a PTS survey was conducted with the objective of confirming the deepest feed zone and the existence of the water level after a successful tie-back job in 2020. Interestingly, the results of the PTS Flowing analysis indicate the presence of a water level at a depth of +1,427 mMD with indications of a steam-liquid mixture. Comparing with the 2015 survey, this survey does not show indications of casing leakage at shallow depths, allowing the conclusion that the 2020 tie-back workover successfully sealed the leakage.

To obtain water chemistry information from the identified water level, a Downhole sampling program was conducted. The Downhole sampling tool used a jarring mechanism with a chamber capacity of 1.500 ml, with sample collection locations at two depths: 1.600 mMD and 1.700 mMD during flowing conditions. The first run at a depth of 1.600 mMD only yielded a 60 ml sample, prompting a second run at a deeper location of 1.700 mMD, resulting in an approximately 800 ml sample with a pH of 5.31 and an electrical conductivity (EC) of 1.520 µS/cm (Figure 6). This sample was then analyzed in the laboratory to determine its type and origin.

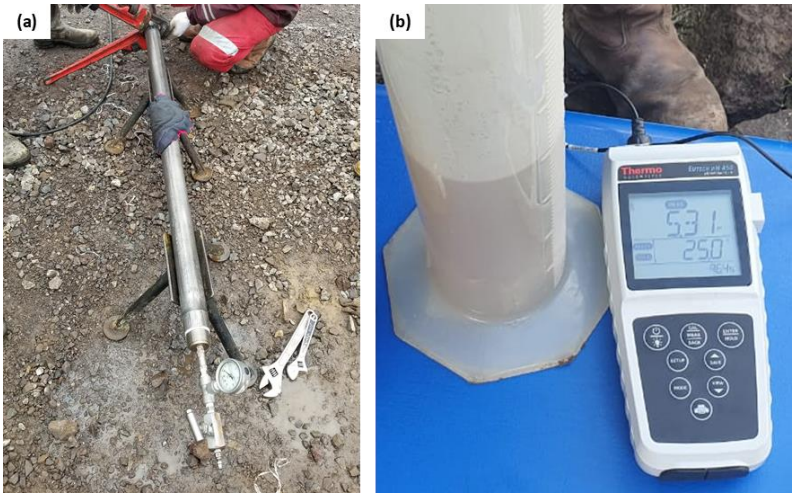

Figure 6. (a) Downhole sampling chamber, (b) Sample collected from DHS at depth 1.700 mMD.

2.2 Presence of water in HND-B

Well HND-B was drilled in 1997 and is the deepest well in Patuha, with an elevation of 350 meters below sea level. This well was subsequently utilized for additional commercial production in 2015 after the first 7 production wells came online in 2014. Positioned with a trajectory toward the southern area of Patuha and relatively away from the central extraction area, it is estimated to be in the peripheral zone. The well shows a dry steam condition at the surface without the presence of water in bottom port sampling, with an enthalpy >2.500 kJ/kg. However, the results of pressure-temperature logging surveys from the initial conditions in 1997 to the latest survey in 2018 consistently indicate a water level at a depth of around 1.670 mMD (Figure 7). Therefore, in June 2021, a downhole sampling program was conducted to determine the chemistry of this water. The downhole sampling tool used a jarring mechanism with a chamber capacity of 1.500 ml, with the target sample collection depth at 1.900 mMD during flowing conditions. A sample was successfully obtained, totaling 1,220 ml with a pH of 8.07 and electrical conductivity (EC) of 3,073 µS/cm, to be further analyzed in the laboratory.

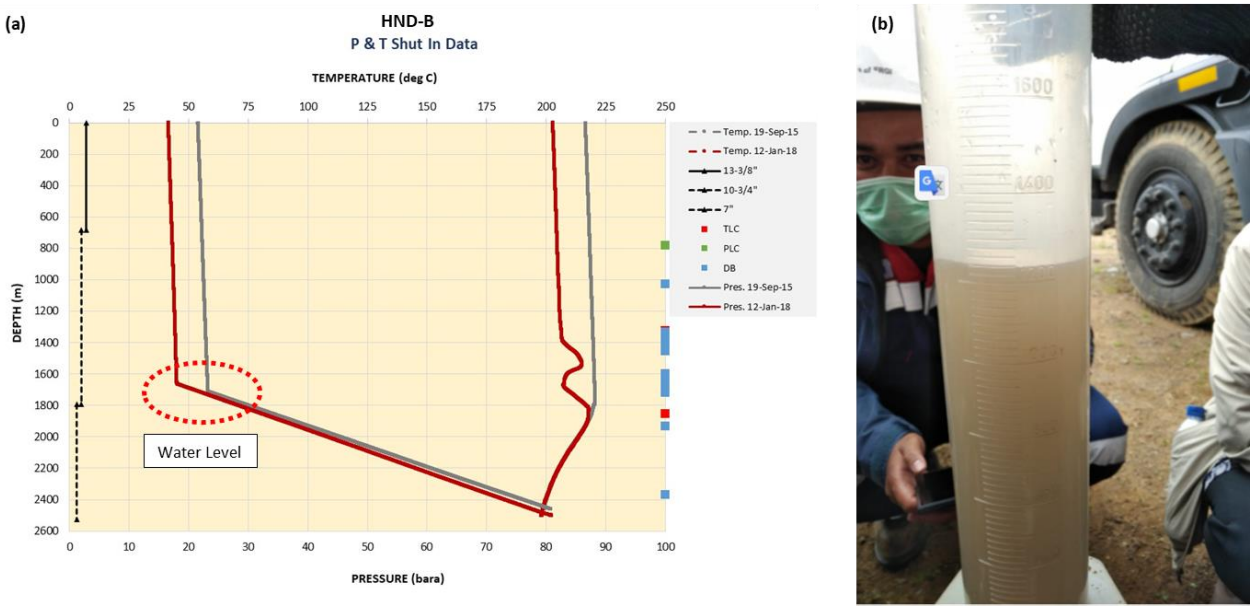

Figure 7. (a) Water level indication based on PT logging surveys in shut-in condition, (b) Sample collected from DHS at depth 1.900 mMD.

2.3 Presence of water in HND-C

Well HND-C was drilled in 1997 in the central part of the field and always gets the center of attention. The well started production in 2015 and showed some unstable behavior compared to the other wells. Since the beginning of production in December 2015, HND-C has been produced using the well washing method in order to maintain steam production. Well washing encompasses water being injected for a certain period. Then, the well is closed until it reaches the maximum WHP before it is produced. From the beginning until 2018, mostly fresh water was used, but after August 2018, condensates with temperature ranging from 35 to 40 deg C were used. Well history shows the problem that causes unstable performance in HND-C is due to the growth of scaling inside the wellbore. Scaling evidence obtained from the well intervention and well monitoring programs shows that the type of scaling is calcite. HND-C has been producing liquid since the beginning of its operation. Based on the Tracer Flow Test (TFT) monitoring, the well has dryness of 95%-99% with a slightly liquid fraction (Table 2).

Table 2. HND-C TFT Results from 2018 – 2021.

Location	Date	FCV (%)	WHP		Steam Rate TFT	Liquid Rate TFT	Enthalpy	TMF	Steam Fraction	Liquid Fraction	Remarks
			psig	barg	t/h	t/h	kJ/kg	t/h			
HND-C	21/02/2018	11	160	11.0	31.0	1.7	2680	32.7	0.95	0.05	with Liquid Fraction
	23/09/2019	11	170	11.7	28.0	1.6	2677	29.6	0.95	0.06	
	18/09/2020	11	123	8.5	43.0	2.4	2669	45.4	0.95	0.05	
	01/04/2021	36	131	9.0	84.7	1.3	2737	86.0	0.99	0.02	

The Separated Water (SPW) sample on the surface showed a very dilute concentration with inconclusive information. This was later confirmed by conducting a liquid Downhole Sampling (DHS), which was suspected to be the trigger for scale deposition after the successful workover cleared the wellbore to 1.679 mMD in December 2020. Downhole Video (DHV) program was carried out during the workover to assess the condition of the wellbore that had experienced scaling growth, along with running downhole sampling at a depth of + 1.423 mMD. The total sample obtained was around + 400 ml with a pH of 8.23 (Figure 8).

To ensure that there was no casing leakage in the shallow area, similar to what occurred in HND-A, a Magnetic Thickness Detector (MTD) survey was conducted to a depth of 843 mMD. The MTD survey results only showed a light corrosion level on the production casing 13-3/8" and casing 20", with no significant metal loss. This condition was also supported by SPW samples from bottom port sampling, indicating low magnesium (Mg) content and suggesting that the produced water originated from condensate. However, geochemical analysis of downhole samples will be more representative in determining the type and origin.

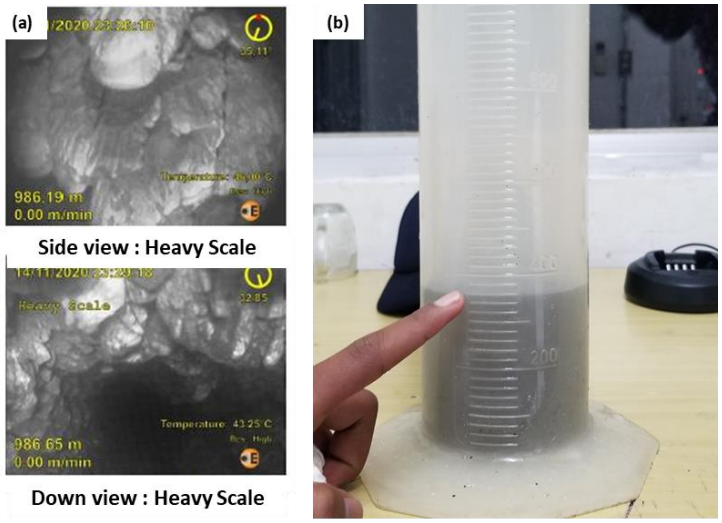

Figure 8. (a) DHV showed scaling calcite inside wellbore, (b) Sample collected from DHS at depth 1.423 mMD.

3. ORIGIN AND PROCESSES

Geochemical monitoring of production wells until 2021 reveals several pieces of evidence indicating the presence of liquid originating from multiple production wells contributing to Unit 1 of the Patuha geothermal field. Previous discussions indicate the confirmation of at least three wells. Data integration from Pressure & Temperature (PT) logging surveys, Magnetic Thickness Detector (MTD), and Downhole Video (DHV), later confirmed by Downhole Sampling (DHS), further strengthens the evidence of liquid presence in these wells, whether partially produced to the surface or remaining "trapped" within the wellbore. In terms of the geochemical monitoring program, collected water samples are then analyzed for evaluation from a geochemical perspective, elucidating their origin and processes.

Below are the results of water sample analysis from wells HND-A, HND-B and HND-C, including both SPW and DHS samples. As supporting data for interpretation, an analysis of river water samples representing groundwater / marginal recharge (MR) samples and condensate from injection wells was also conducted. Water sample analysis parameters include dissolved elements (anions and cations) and stable isotopes (Table 3).

Table 3. Water analysis for HND-A, HND-B and HND-C with supporting data.

HND-A (BEFORE WORKOVER)																					
Sampel	Date	EC	TDS	pH (Field)	pH (Lab)	Li	Na	K	Ca	Mg	SiO_2	B	Cl	F	SO_4	HCO_3^-	NH_4^+	As	Fe	del ^{18}O	del D
		µS/cm	ppm			ppm															
HND-A (SPW)	24-Oct-18	132	-	8.75	-	0.028	5.84	3.760	11.90	4.18	81.5	0.42	0.92	0.12	40.9	21	0.1	0.015	0.013	N/A	
	27-Sep-19	127	150	6.79	6.04	0.012	5.97	3.41	10.40	3.32	63.3	0.35	0.72	0.09	43.7	19.1	0.16	0.01	0.015		
	09-Sep-20	-	146	6.63	5.95	0.013	6.02	2.95	9.75	3.12	63.9	0.25	1.00	0.07	39.2	19.3	0.198	0.024	0.011	-6.97	-48.9
HND-A (AFTER WORK OVER)																					
Sampel	Date	EC	TDS	pH (Field)	pH (Lab)	Li	Na	K	Ca	Mg	SiO_2	B	Cl	F	SO_4	HCO_3^-	NH_4^+	As	Fe	del ^{18}O	del D
		µS/cm	ppm			ppm															
HND-A (SPW)	17-Dec-20	20.5	16.9	-	5.35	0.01	0.06	0.08	0.57	1.15	4.25	4.98	0.27	1.30	3.94	2	0.43	0.01	0.24	-4.03	-38.3
	30-Mar-21	193	26.6	6.30	5.21	0.01	0.93	0.69	1.18	0.28	10.30	6.38	1.95	1.63	2.77	2	0.87	0.08	0.26	N/A	
HND-A (DHS) @1700 mMD	12-Jul-21	1520	1460	5.31	4.91	0.32	246.00	27.30	27.40	1.32	528.00	2.67	54.90	2.21	560	2	0.34	0.29	8.17	-3.29	-35.3

HND-B (DHS)																					
Sampel	Date	EC	TDS	pH (Field)	pH (Lab)	Li	Na	K	Ca	Mg	SiO_2	B	Cl	F	SO_4	HCO_3^-	NH_4^+	As	Fe	del ^{18}O	del D
		µS/cm	ppm			ppm															
HND-B (DHS) @1900 mMD	29-Jun-21	2850	1890	8.07	6.5	1.82	521	58.5	23.8	0.142	251	49.30	676	13.40	241	46.2	3.15	5.84	0.562	-4.98	-37.9

HND-C (BEFORE WORKOVER)																					
Sampel	Date	EC	TDS	pH (Field)	pH (Lab)	Li	Na	K	Ca	Mg	SiO_2	B	Cl	F	SO_4	HCO_3^-	NH_4^+	As	Fe	del ^{18}O	del D
		µS/cm	ppm			ppm															
HND-C (SPW)	08-Jun-18	282	345	5.54	6.22	0.03	23.60	5.84	23.50	0.01	198	4.13	28.80	2.77	34.40	23.20	1.21	0.20	0.04	N/A	
	29-Oct-18	177	-	8.51	-	0.02	29.90	6.33	5.74	0.11	137	3.55	3.19	1.12	31.20	58.40	0.10	0.03	0.15		
	23-Sep-19	283	237	6.32	5.93	0.01	21.30	5.10	31.20	0.03	78	5.39	61.40	2.26	11.70	20	0.91	0.02	0.06	-3.84	-40.9
	18-Sep-20	171	232	7.10	6.06	0.02	23.00	4.85	8.44	0.01	121	7.29	3.70	1.85	26.20	35.20	0.57	0.01	0.02	N/A	
HND-C (AFTER WORKOVER)																					
Sampel	Date	EC	TDS	pH (Field)	pH (Lab)	Li	Na	K	Ca	Mg	SiO_2	B	Cl	F	SO_4	HCO_3^-	NH_4^+	As	Fe	del ^{18}O	del D
		µS/cm	ppm			ppm															
HND-C (DHS) @1423 mMD	11-Dec-20	518	557	8.20	6.50	0.03	43.00	9.20	52.20	0.36	204.00	10.10	5.61	4.79	170	55.70	0.10	0.27	0.17	-0.4	-22.1
HND-C (SPW)	12-Dec-20	147	201	6.11	6.04	0.01	19.30	3.95	9.09	0.10	89.80	5.63	1.69	1.31	34.60	35.50	0.42	0.10	0.02	-3.9	-38.5
	01-Apr-21	153.2	230	6.75	6.03	0.03	22.60	4.63	6.01	0.01	107.00	13.00	2.56	2.17	39.60	31.90	0.56	0.22	0.02	N/A	

CIPAKU RIVER																					
Sampel	Date	EC	TDS	pH (Field)	pH (Lab)	Li	Na	K	Ca	Mg	SiO_2	B	Cl	F	SO_4	HCO_3^-	NH_4^+	As	Fe	del ^{18}O	del D
		µS/cm	ppm			ppm															
Cipaku River	17-Dec-20	-	58.8	5.75	-	0.01	2.59	1.63	6.04	1.69	23.3	0.1	2.05	0.021	5.43	15.9	0.1	0.01	0.047	-8.52	-53.4

CONDENSATE INJECTION																					
Sampel	Date	EC	TDS	pH (Field)	pH (Lab)	Li	Na	K	Ca	Mg	SiO_2	B	Cl	F	SO_4	HCO_3^-	NH_4^+	As	Fe	del ^{18}O	del D
		µS/cm	ppm			ppm															
HND-X	17-Dec-20	-	75.7	-	5.51	0.01	19.4	0.085	0.978	0.206	1.54	0.697	0.363	-	52.4	2	5.85	-	-	0.28	-3.9

Basic water geochemical evaluation was conducted using anion and cation diagrams. The Anion Cl-SO_4-HCO_3 diagram (Figure 9.a) was used to determine the water type originating from SPW samples from bottom port sampling in wells HND-A & HND-C (surface) and DHS samples from wells HND-A, HND-B & HND-C.

Plot results of the HND-A SPW sample, before and after workover (WO) tie-back casing using the trilinear Cl-SO_4-HCO_3 consistently remain in the SO_4 water area, with a slight shift in the after WO samples. This is due to changes in concentration from the after WO samples, which indicate the typical condensate fluid characterized by a decrease in sulfate content and other dissolved elements, and without experiencing mixing with surface water influx. This condition was clear from the decreased concentration of Mg (Table 3), confirming the success of the WO tie-back casing program on this well. Furthermore, the analysis results of the DHS sample at a depth of 1.700 mMD (after WO) show different concentrations compared to SPW samples, with higher concentrations of dissolved elements, predominantly SO_4 causing the plot closer to the apex SO_4 area.

The plot results of the SPW samples from well HND-C until 2020 (before WO tie-back casing) showed inconsistent patterns. However, data from 2020 to 2021 indicate a trend shifting towards SO_4. In contrast to the SPW samples from well HND-A, which demonstrate typical condensate characteristics with low concentrations of dissolved elements, the SPW samples from well HND-C show higher concentrations of dissolved elements. Additionally, this well has experienced scaling deposition inside the wellbore with the main root cause being the presence of liquid. Consequently, a DHS program is proposed to obtain representative samples and explain the deposition mechanism of calcite scaling inside the wellbore. The plot results of the DHS data at a depth of 1,422 mMD show a shift toward the apex of SO_4.

Well HND-B is classified as a dry steam well, nevertheless consistent indications of a water level from logging data prompted the decision to conduct a DHS. The plot results of the anion diagram Cl-SO_4-HCO_3 reveal that well HND-B exhibits a distinguished water type compared to the DHS samples from wells HND-A and HND-C, which belong to the SO_4 water type. The plot results of well HND-B indicate a shift towards the chloride (Cl) water area, typically suggesting a brine reservoir type. Supporting data from HND-X as an injection well and the Cipaku river do not indicate any similarity in terms of chemistry, suggesting that the water found in wells HND-A, HND-B, and HND-C may not have a direct correlation

The Na-K-Mg cation ternary diagram used to determine fluid equilibrium is shown in Figure 9.b. The plotted results reveal that water samples from wells HND-A and HND-C (SPW & DHS) is categorized as immature water, denoting a non-reservoir fluid. An intriguing observation emerges with well HND-B, as its water sample uniquely exhibits partial equilibration. This distinctive condition aligns with findings from the anion diagram plot, placing it within the Cl water area.

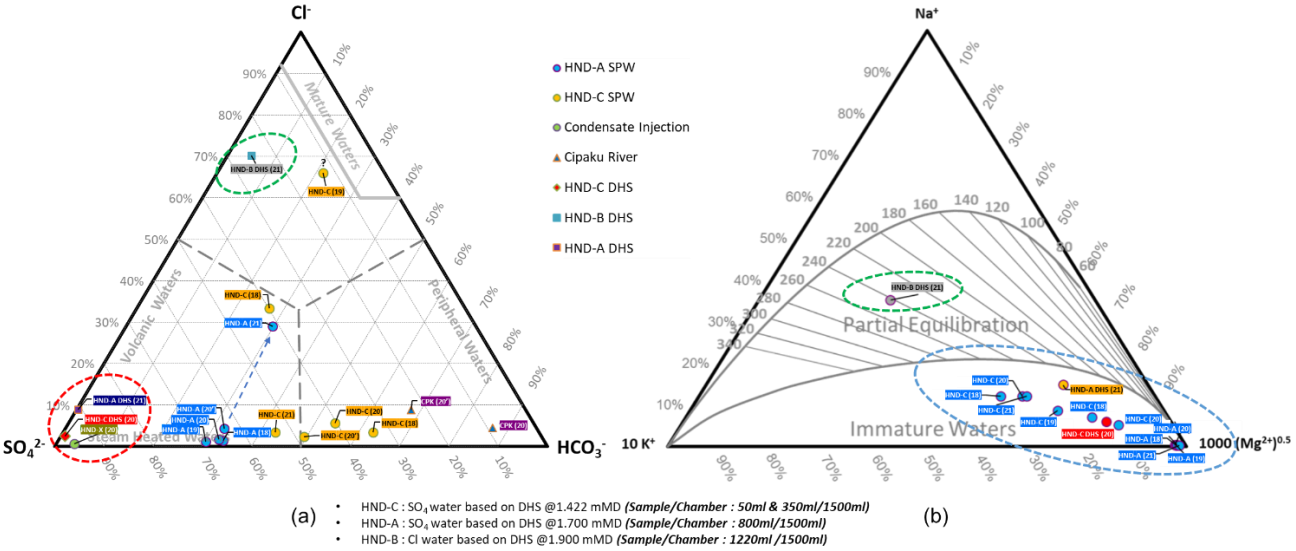

Figure 9. Ternary diagram: (a) Anion and (b) Cation

Among the three DHS samples, only wells HND-A and HND-B clearly showed the water level profile from the logging survey results. However, for well HND-C, the thickness of the water level cannot be confirmed due to tagging issues during the survey, preventing reaching the total depth (TD). Subsequently, a comparison of chemistry was conducted among these three DHS samples (Figure 10). DHS samples HND-A and HND-C, based on earlier explanations are confirmed as SO_4 water type (secondary water). Nevertheless, these two samples show slight differences in their chemistry. DHS sample HND-A has a relatively lower pH value and higher concentrations of SO_4, SiO_2, and Fe, with lighter stable isotope values compared to DHS sample HND-C. This condition may arise from differences in the intensity of water-rock interaction, leaching of rocks, and physical processes such as boiling during fluid traveling, thereby affecting the values of some elements and stable isotopes in both wells. It is observed in well HND-C that the neutralization process occurs as the fluid travels, characterized by an increase in SiO_2 and Ca concentration with a neutral pH. This condition also contributes to the deposition of calcite scaling. Stable isotope analysis of DHS indicates an enrichment process compared to the other wells, marked by ^{18}O shifting towards heavy isotopes with a minor shift of ^{2}H. This condition suggests that this liquid had sufficient time to react with the reservoir rock. Additionally, the dominant lithology intersecting HND-C in the reservoir was diorite with moderate silica content. On the other hand, the DHS sample from HND-B with relatively high Cl, Na, and K values is suspected to originate from a residual liquid in the rock matrix that has started to carry over.

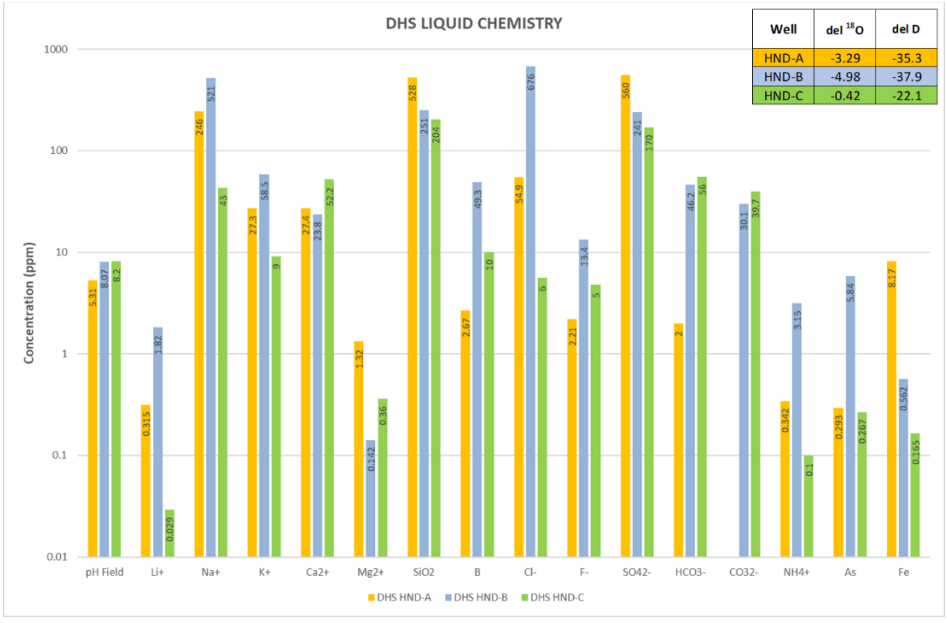

Figure 10. Comparison of DHS samples from wells HND-A, HND-B & HND-C.

Stable isotopes ^{18}O and ^{2}H data were also evaluated using samples of steam condensate (SCS) isotopes and water isotopes from HND-A, HND-B, and HND-C (SPW & DHS samples), as well as condensate injection from well HND-X and Cipaku river. The Local Meteoric Water Line (LMWL) equation used refers to the LMWL equation of Java Island (Abidin & Wandowo, 1995), which was then validated with the isotopic values of the Cipaku river. Data from well HND-A in 2020 briefly showed a trend of increasing lighter stable isotopes (lower isotopic values) before returning to normal in 2021. This trend was influenced by the mixing with a non-reservoir fluid influx that was more diluted due to leakage issues on production casing (before the tie-back casing). As discussed earlier, Separated Water (SPW) samples obtained showed typical meteoric water characteristics with high Mg. Isotope plots from DHS samples of wells HND-A and HND-B, as well as SPW samples from wells HND-A and HND-C, were relatively positioned on a single mixing line with the DHS sample from well HND-C as the end member. Typically, condensate injection wells are plotted as the end member, undergoing enrichment due to the evaporation process in the cooling tower. However, in this case, the isotopic results of condensate injection tend not to fall on the same mixing line. This is also consistent with the results of a previous reservoir tracer test, where it can be concluded that the majority of the injection flows away from/out of the production well area (Figure 11).

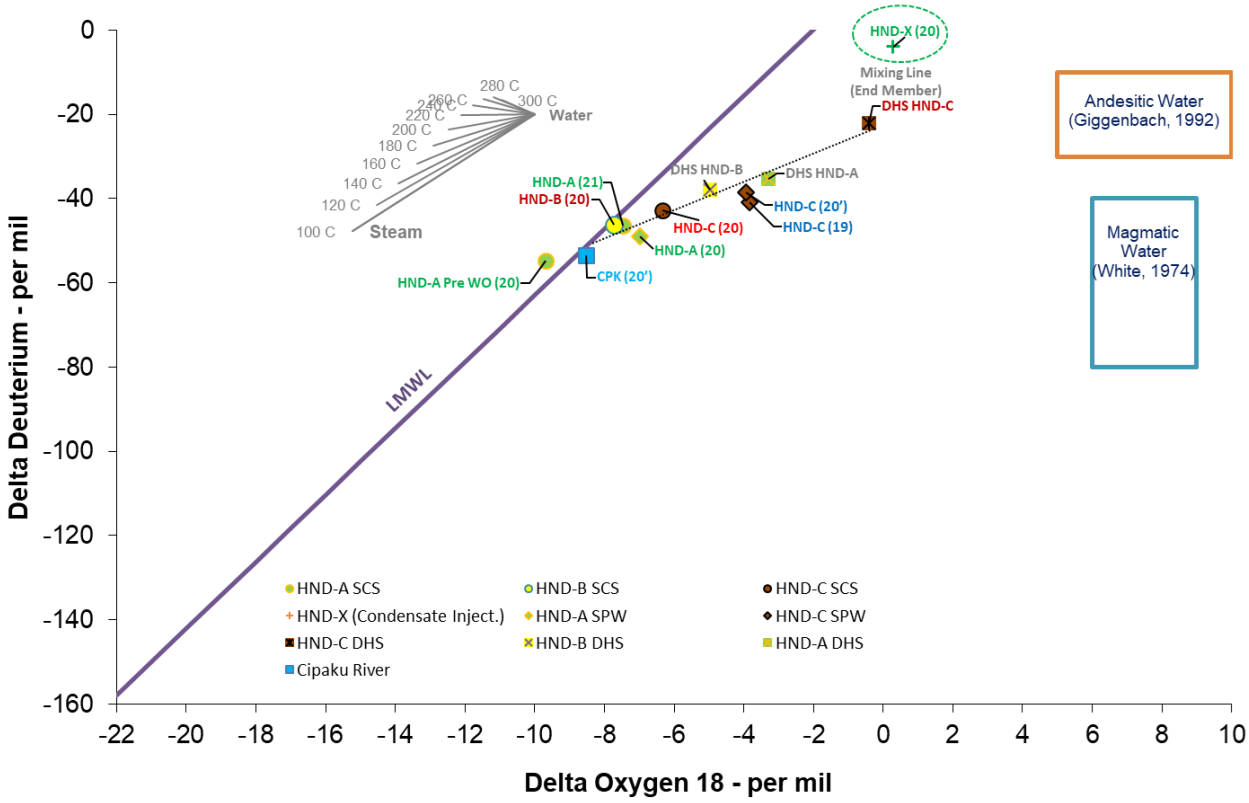

Figure 11. Stable isotope graphs from production well samples (SCS, SPW & DHS), injection well, and meteoric water.

Furthermore, the utilization of gas data in the FT-HSH2 (pyrite-hematite equilibrium reaction) geothermometer can also reveal trends in the steam fraction. The FT-HSH2 gas geothermometer exhibits slightly different plot results in wells HND-A and HND-B compared to other wells, with a tendency towards a lower steam fraction in these two wells. The cause of this condition is not yet clearly known but is closely correlated with the history of water level encounters in wells HND-A and HND-B. This condition aligns with the plot results of the H_2-H_2S-CH_4 gas diagram, indicating that wells HND-A and HND-B shift towards H_2S, signifying the influence of the quenching process (Figure 12.a). Implementation of the FT-CO_2 gas geothermometer also reveals that wells HND-A & HND-B consistently display lower steam fraction values, akin to the indications of the FT-HSH2 geothermometer (Figure 12.b).

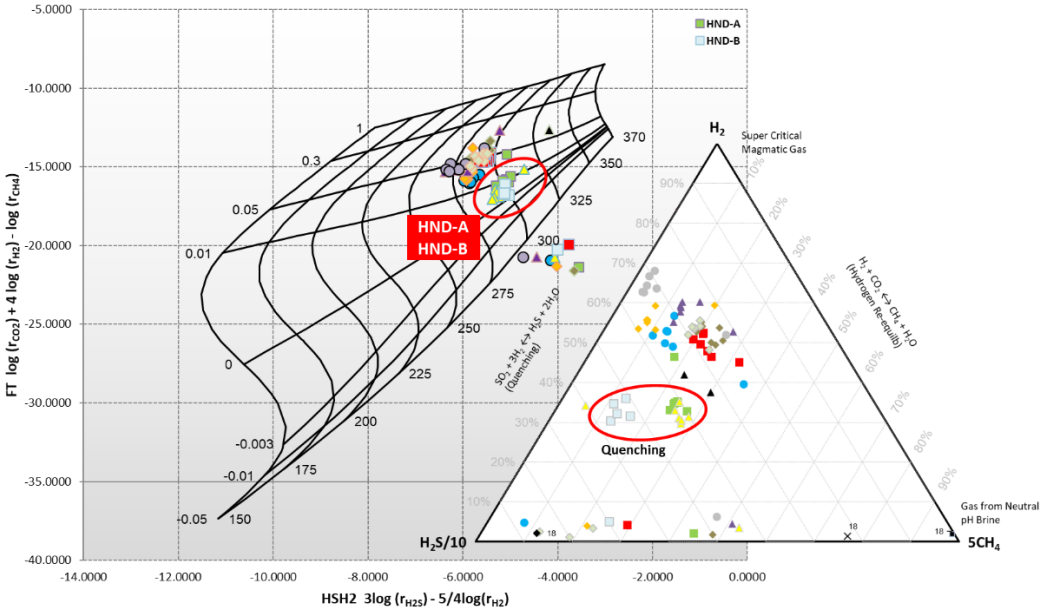

(a)

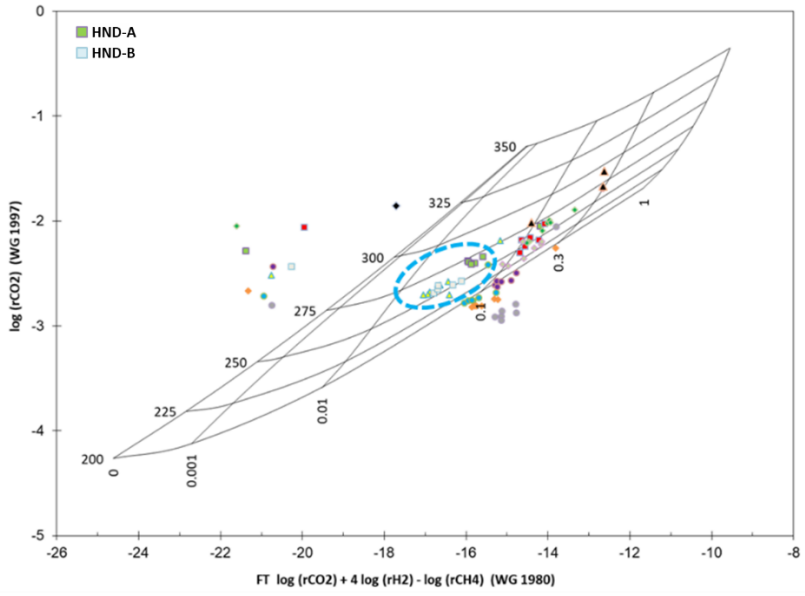

(b)

Figure 12. Gas Geothermometer: (a) FT-HSH2 - Diagram H_2-H_2S-CH_4 & (b) FT-CO_2.

The SO_4 water from the downhole sample of well HND-C is believed to have originated from a condensation process occurring in a shallower zone. This condensation zone subsequently gives rise to a steam-condensate layer around the clay cap. This conceptualization aligns with the model of a vapor-dominated geothermal system proposed by White et al. (1971) (Figure 13), drawing parallels with the Geyser and Lardarello fields, where the condensate layer was positioned above the steam zone. Similar to Kamojang, the reservoir is capped by a steam-heated layer (Schubert & Straus, 1980) (Utami, 2000). The water in the upper part of this layer manifests as steam condensate with an acid sulfate composition (Healey & Mahon, 1982).

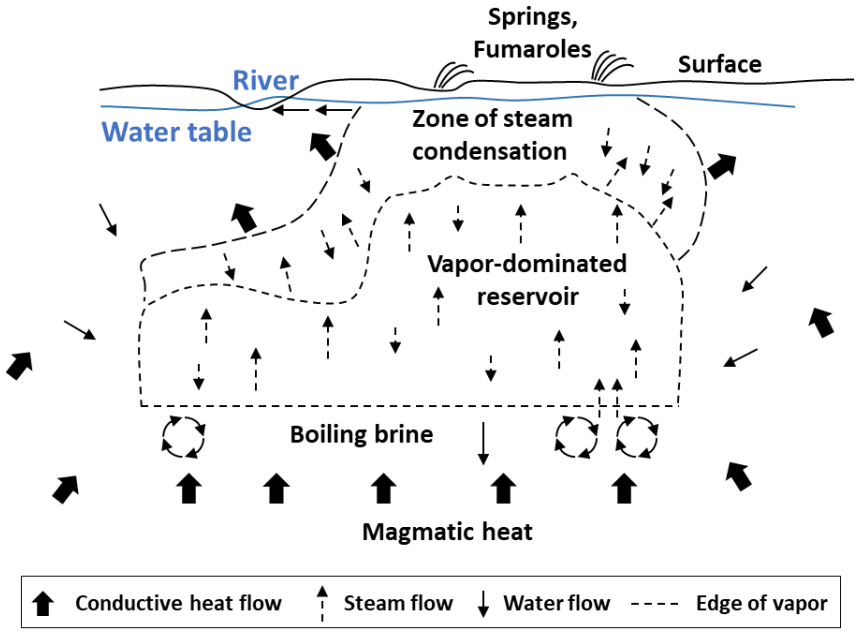

Figure 13. Conceptual model of vapor-dominated geothermal systems by White et al. (1971).

An alternative model from a distinct perspective elucidates the chemical distribution (non-condensable gas concentration) in a shallow section of a vapor-dominated reservoir by introducing effects of conductive heat loss through the cap rock (D'Amore and Truesdell, 1979) (Figure 14). They observed that water vapor in geothermal steam may condense if there is conductive heat loss through the cap rock, while non-condensable gases may not condense, remaining in the steam. Consequently, gas concentration increases toward the margin of the reservoir from its center along its flow (Hanano, 2010).

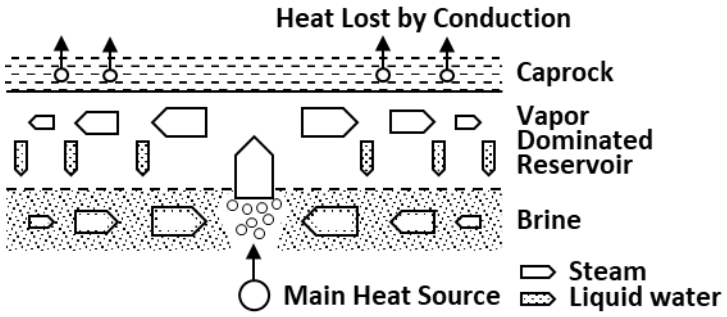

Figure 14. Conceptual model of a vapor-dominated geothermal reservoir by D'Amore and Truesdell (1979).

The process of liquid formation in well HND-A may occur with a similar mechanism but with different intensities of water-rock interaction and permeability control, resulting in a more distinct water level pattern. Concerning the DHS water in well HND-B, which displays chloride water followed by relatively high Cl, Na, and K values, it is suspected to originate from residual liquid in the rock matrix that has started to carry over. This liquid then fills the wellbore and becomes 'trapped water' due to tight permeability conditions without a feed zone, preventing it from flowing upward. Nevertheless, there is a lack of confirmation regarding whether this well has penetrated deep reservoir brine, given its status as the deepest production well in Patuha, with no comparable well at the same elevation.

4. LONG-TERM EFFECT

Collected data during the HND-C well intervention and well monitoring program concluded that scaling growth was already occurring inside the wellbore. This led to some unstable behavior, such as a rapid drop in WHP and flow rate compared to the other wells. In 2018, HND-C showed scaling evidence inside the wellbore, as observed from the scale catcher and later confirmed by X-Ray Diffraction (XRD) analysis to be Calcite. The Downhole Video (DHV) Survey provides a clearer visual of the wellbore condition covered by calcite scaling on the 10-3/4" perforated liner (Figure 15).

Root cause analysis indicates that scaling deposition in HND-C is caused by the flashing of the liquid fluid inside the wellbore. The liquid originates from the steam-condensate layer with a lower temperature and greater density, allowing it to percolate downward to the bottom of HND-C (Sujarmaitanto et al., 2022). The neutralization process occurs as the fluid travels, characterized by an increase in SiO_2 and Ca

concentration with a neutral pH. Flashing of the liquid fluid inside the wellbore triggers the following chemical reaction: $Ca^{+2} + 2HCO_3^- \Leftrightarrow CaCO_{3,s} + CO_2 \uparrow + H_2O$, causing the deposition of calcite scaling.

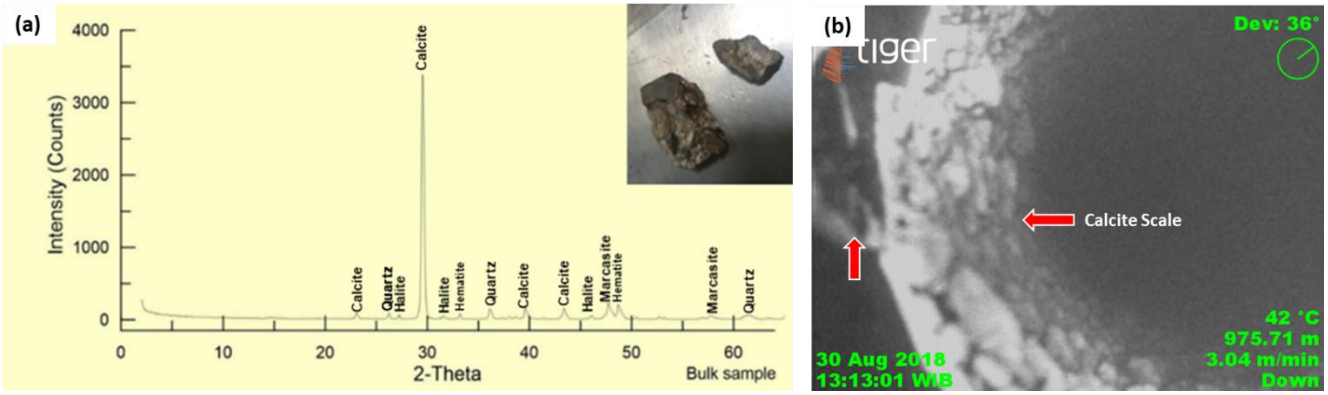

Figure 15. Calcite scaling evidence: (a) XRD analysis, (b) Calcite scale started developed at depth 975 mMD (perforated liner).

The occurrence of scaling within the wellbore is also noted in well HND-A (prior to the tie-back casing installation). Scaling samples were retrieved at a depth of 1950 mMD during the execution of the 5.5" well clearance operation on August, 2020 (Figure 16). These samples underwent analysis using the Scanning Electron Microscope-Energy Dispersive Spectroscopy (SEM-EDS) method for mineralogy identification (Herdianita, 2020).

The SEM-EDS analysis results indicate that the developed scaling is magnesium silicate (Figure 17). This scaling illustrates the impact of mixing from shallow groundwater (with a relatively high Mg content) with geothermal fluids, subsequently heated, leading to precipitation (Gunnlaugsson, 2014). The suspected occurrence of this scaling aligns with the period when the casing of well HND-A was likely experiencing leakage (casing leakage) at a relatively shallow elevation. During that time, the condition of well HND-A briefly displayed a dryness value of approximately 50%, necessitating additional surface facilities like a separator. Furthermore, a critical aspect is that failure to promptly address the presence of this substantial liquid volume could pose a risk of steam collapse.

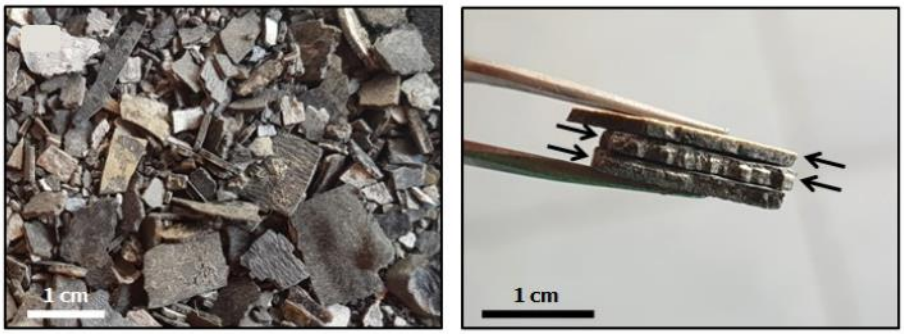

Figure 16. Scaling samples from HND-A (before tie-back casing).

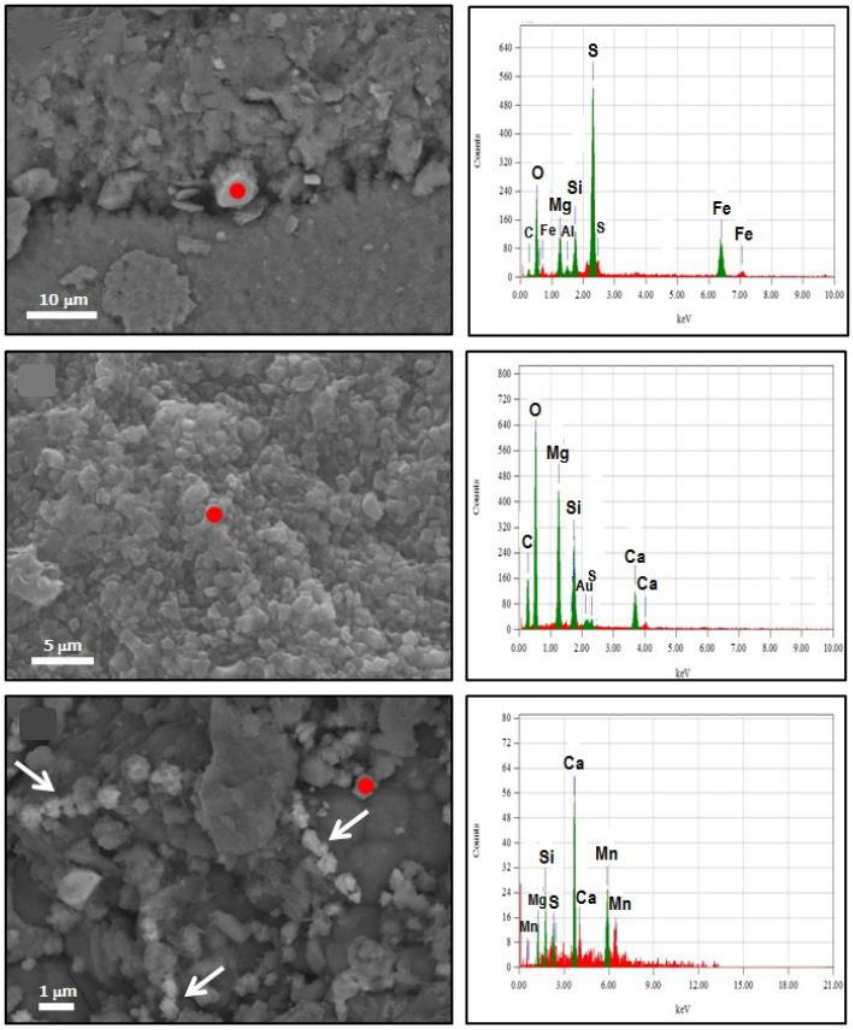

Figure 17. Results of SEM-EDS analysis indicate Magnesium silicate.

4. CONCLUSION

Some wells in Patuha have shown the presence of liquid, visually observed through the sampling port at the bottom during routine geochemical sampling. Data integration is conducted in this evaluation, incorporating information from Pressure & Temperature (PT) logging surveys, Downhole Video (DHV), Downhole Sampling (DHS), Magnetic Thickness Detector (MTD), and geochemical analysis. Based on the history and evidence regarding the presence of liquid, three wells have been confirmed: HND-A, HND-B, and HND-C. The evaluation of the origin and processes of each sample obtained indicates that the water samples from wells HND-A & HND-C are SO_4 water originating from the steam-condensate layer around the clay cap that has undergone water-rock interaction, leaching of rocks, and physical processes such as boiling during fluid traveling with varying intensity. On the other hand, the water sample from well HND-B shows chloride water and is suspected to originate from residual liquid in the rock matrix that has started to carry over. This liquid then fills the wellbore and becomes 'trapped water' due to tight permeability conditions without a feed zone, preventing it from flowing upward. Nevertheless, there is a lack of confirmation regarding whether this well has penetrated deep reservoir brine, given its status as the deepest production well in Patuha, with no comparable well at the same elevation. Ultimately, the existence of this liquid requires special attention, particularly considering its potential long-term effects, as it may impact the performance and sustainability of production wells.

ACKNOWLEDGEMENTS

The author would like to thank the management of PT Geo Dipa Energi (Persero) for permission to publish this work.

REFERENCES

Abidin, Z., Wandowo.: Isotope study in geothermal fields in Java Island. In: Proceeding of the Final Research Coordination Meeting on the Application of Isotope and Geochemical Techniques to Geothermal Exploration in the Middle East, Asia, the Pacific and Africa Held in Dumaguete City, Philippines, 12-15 October 1993. International Atomic Energy Agency, (1995) Vienna Austria, pp. 83-91.

D'Amore, F. nd Truesdell, A.H. (1979) Models for steam chemistry at Lardarello and The Geysers. Proceedings of the 5th Workshop on Geothermal Reservoir Engineering, Stanford University, (1979), 283-297.

Gunnlaugsson, E. et al.: Problems in Geothermal Operation – Scaling and Corrosion. Santa Tecla, El Salvador (2014).

Hanano, M.: Improvement of Understanding of Vapor-dominated Geothermal Resources (2010).

Healey, J. and Mahon, W.A.J.: Kawah Kamojang Geothermal Field, West Java, Indonesia. Proc. Pacific Geothermal Conference incorporating the 4th New Zealand Geothermal Workshop. Vol.2, The University of Auckland, (1982), pp.313-319.

Herdianita, N. R.: Report on Priority Samples from PPL-2. PT. Geo Dipa Energi (Persero), Internal Report., Jakarta (2020).

Schubert, G. & Straus, J. M.: Gravitational stability of water over steam in vapor-dominated geothermal systems. *Solid Earth, Journal of Geophysical Research,* Volume 85, (1980), pp. 6505-6512.

Sujarmaitanto, H. et al.: Calcite Scaling in Vapor-Dominated Well, Patuha Geothermal Field, 8th Indonesia International Geothermal Convention & Exhibition, Jakarta (2022).

Utami, P.: Characteristics of The Kamojang Geothermal Reservoir (West Java). Kyushu-Tohoku, Japan, World Geothermal Congress (2000).

White, D. E., Muffler, L. J. P. & Truesdell, A. H.: Vapor-Dominated Hydrothermal Systems Compared with Hot-Water Systems. *Economic Geology Vol. 66*, (1971), pp. 75-97.